Surface Density Dependence of PCR Amplicon Hybridization on PNA/DNA Probe Layers

Danfeng Yao,* Junyoung Kim,* Fang Yu,* Peter E. Nielsen,† Eva-Kathrin Sinner,*‡ and Wolfgang Knoll*
*Max-Planck-Institute for Polymer Research, Mainz, Germany; †Panum Institute, IMBG, Department of Biochemistry B, Copenhagen N, Denmark; and ‡Max-Planck-Institute of Biochemistry, Munich, Germany

ABSTRACT Surface plasmon field-enhanced fluorescence spectroscopy was employed to extensively investigate the hybridization behaviors of polymerase chain reaction (PCR) amplicons on a peptide nucleic acid (PNA) or DNA probe layer that was previously attached on a streptavidin-modified gold surface via biotin/streptavidin interaction. Despite the neutral backbone of PNA, the hybridization reactions were strongly influenced by the variation of ionic strength. The association rates exhibited a monotonic decrease with ionic strength increase and the maximum hybridization signal was achieved at an intermediate sodium concentration (~100 mM). These effects were mainly ascribed to the electrostatic cross talk among the hybridized DNA molecules and the secondary structure of PCR amplicons. For the negatively charged DNA probes, the hybridization reaction was subjected additionally to the DNA/DNA electrostatic barrier, particularly in lower ionic strength range (e.g., 10 ~ 150 mM Na^+). The electrostatic cross talk was shown to be largely reduced if the PNA probe layer was sufficiently diluted by following a strategic templated immobilization method. As a consequence, a pseudo-first-order kinetic model was applicable to describe the hybridization kinetics, and affinity constants were derived for evaluating the influence of single nucleotide polymorphisms (SNPs).

INTRODUCTION

The analysis of polymerase chain reaction (PCR) products (or genomic DNA) is in the main focus of nucleic acid-based biosensor and biochip development. The applied methodologies typically rely on the hybridization of PCR amplicons to surface-attached probe DNA (or DNA analogs) and the readout of the binding reaction by, e.g., fluorescence techniques (Epstein et al., 2002), or by measuring inherent physical parameters of the DNA analytes (Bier et al., 1997; Yang et al., 1997). The surface hybridization of PCR amplicons is rather complex, which experiences an environment substantially different from that in a homogeneous phase. As reported by Southern et al. (1999), the solid support may sterically interfere with the hybridization reaction, although the interference can be alleviated by introducing ''arms'' between the surface and the probes. Additionally, the confinement of probes on the surface significantly limits the space for the occurring of hybridization, leading to interaction between adjacently bound molecules both sterically and electrostatically. The longer the PCR amplicons are, the more severe the interaction is. Therefore, the corresponding hybridization kinetics can be very complex, dominated not only by the affinity of the recognition sequences (selective fragments) but also by those surface effects. Consequently, the description and understanding of the hybridization kinetics are so far very limited, although they are of great significance in the in-depth investigation of the hybridization mechanism, and provide opportunities of controlling the hybridization process, e.g., in the application of evaluating and developing new antisense drugs based on microarray technologies.

It has been pointed out that the surface effects could be efficiently reduced by decreasing the probe density in oligonucleotide hybridization (Herne and Tarlov, 1997; Yu et al., 2004). However, the price paid is a substantially reduced binding volume and is practically unaffordable for most of the reported biosensing techniques, particularly in the case of PCR amplicon hybridization. In view of this, surface plasmon field-enhanced fluorescence spectroscopy (SPFS) was employed in this work for the study of PCR amplicon hybridization. SPFS is a newly developed biosensing technique based on the surface plasmon resonance phenomenon (Liebermann et al., 2000). Compared to the incident field, the evanescent field of a surface plasmon is enhanced by a factor of 16 for a gold/water interface at the respective resonance angle and then decays evanescently into the dielectric medium, with a wavelength dependent penetration depth of approximately $L_Z = 150$ nm. The enormously enhanced electromagnetic field can excite fluorophores placed within its evanescent tail, resulting in a strong fluorescence signal. Based on that, SPFS has demonstrated excellent sensitivity and performance in the quantitative analysis of antibody-antigen interaction (Yu et al., 2004), where the binding events relating to a few molecules can be resolved.

Here, oligonucleotides or peptide nucleic acids (PNAs) were used as the surface-attached probes for PCR amplicon hybridization. Modified with a biotin moiety at the 5′-end or the N-terminus, the oligonucleotide or PNA probe can be

Submitted August 20, 2004, and accepted for publication January 14, 2005.
Address reprint requests to W. Knoll, Max-Planck-Institute for Polymer Research, Ackermannweg 10, 55128, Mainz, Germany. Tel.: 49-6131-379-160; Fax: 49-6131-379-360; E-mail: knoll@mpip-mainz.mpg.de.

0006-3495/05/04/2745/07 $2.00
doi: 10.1529/biophysj.104.051656

assembled on the streptavidin (SA)-modified gold surface via biotin/SA interaction. PNA is a DNA mimic in which the negatively charged phosphate deoxyribose backbone is replaced by a neutral *N*-(2-aminoethyl) glycine linkage (Egholm et al., 1993). In view of the different electrostatic nature of PNA and DNA backbone, the ionic strength dependence of PCR amplicon hybridization on the two kinds of probe layers were explored, respectively. To eliminate the surface effects, a templated immobilization strategy was proposed, by which a homogeneous PNA probe layer with ~40-fold dilution was achieved. The surface dilution simplifies the hybridization kinetics and provides us with the possibility of an in-depth quantitative analysis. In this work, the hybridization behaviors of PCR amplicons were systematically studied on both diluted and undiluted probe layer.

MATERIALS AND METHODS

Preparation of PCR amplicons

The forward and reverse primers (MWG-Biotech, Ebersberg, Germany) were both 30-base oligonucleotides, as shown in Table 1. The forward primer was labeled by Cy5 at the 5′-end for the SPFS measurement. Recombinant plasmids (~4 kb) were used as templates for the PCR amplification. PCR amplification was performed in a thermocycler (Biometra, Goettingen, Germany). Reagents for each 50 μl reaction volume included: 5 units of *Taq* polymerase (Amersham Biosciences, Uppsala, Sweden), 1 × PCR buffer (Amersham Biosciences), 60 pmol of the forward primer and 80 pmol of reverse primer, 0.2 mM dNTPs (Fermentas, St. Leon-Rot, Germany), and 100 ng of the plasmid DNA. After an initial denaturation at 96°C for 1 min, each of the 30 cycles of amplification consists of 30 s of template denaturation at 96°C, 30 s of primer annealing at 50°C and 30 s of primer extension at 72°C.

The resulting PCR amplicons (T1 and T2) were then purified by ethanol precipitation. For 50 μl PCR samples, 125 μl ethanol (Sigma, St. Louis, MO), and 5 μl of 3 M sodium acetate (Sigma) were added. The mixture was shaken, and then kept at −20°C for more than 6 h to induce precipitation. The PCR amplicons were collected by centrifugation at 16,000 × *g* for ~0.5 h. Composed of 196 bp, the PCR amplicons T1 and T2 differ from each other by a one-base substitution (T/C) in the 15-base recognition sequence (see Table 1).

TABLE 1 Sequences of all PNA and DNA strands used in this work

Name	Type	Sequence
P2	PNA	NH_3-Biotin-$(egl)_9$-TGTACATCACAACTA-COOH
P2	DNA	5′-Biotin-$(TTT)_5$-TGTACATCACAACTA-3′
T75*	DNA	5′-Cy5-$(TTT)_{10}$-TAGTTGTGATGTACA-$(TTT)_{10}$-3′
Forward primer	DNA	5′-Cy5-GTACCGAGCTCGGATCCACTAG-TAACGGCC-3′
Reverse primer	DNA	5′-GCCGCCAGTGTGATGGATATCTGCA-GAATT-3′
Sense strand of T2	DNA	5′-Cy5-. . . . . TAGTTGTGATGTACA . . . . . -3′
Sense strand of T1	DNA	5′-Cy5-. . . . . TAGTTGTGACGTACA . . . . . -3′

The PCR amplicons underwent the following denaturation process before the biosensing studies, unless otherwise stated: the heat denaturation is composed of three steps, heating the DNA sample (in 10 mM PB buffer) at 96°C for 10 min, quickly quenching it to 0°C in an ice-water mixture and returning to room temperature (RT).

Preparation of an undiluted PNA or DNA probe layer

A mixed self-assembled monolayer (SAM) of biotinylated thiols (synthesized in our group) and OH-terminated thiols (Sigma) was prepared on the Au-coated glass substrates ($d_{Au} = 50$ nm) via Au-sulfur bonding. The ratio of the two thiols (1:9) has been optimized in previous work to obtain the largest coverage of streptavidin (SA) (Spinke et al., 1993). The biotinylated PNA P2 (synthesized in our group) or DNA P2 (MWG-Biotech) was then immobilized on the substrates by interacting with the tetrameric SA molecules (see Fig. 1 *A*). PNA P2 and DNA P2 contain identical 15-base sequences, which are fully complementary to the recognition unit of the sense strand of the PCR T2. The buffer used in this work contained 10 mM phosphate buffer (PB, pH 7.4), with 0.005% Tween 20 and 2 mM EDTA. High sodium concentrations were obtained by adding sodium chloride.

Preparation of a diluted PNA probe layer

To obtain a diluted PNA probe layer, PNA P2 (300 pM) was mixed with T75* (see Table 1, MWG-Biotech) at a molar ratio of 1:10 in 10 mM phosphate buffer (PB). After being incubated at RT for ~2 h, the mixture was injected into the flow cell with the substrate exposing the SA layer. The binding was stopped after ~4 min by replacing the mixture with buffer. A diluted PNA probe layer was then formed by the removal of the T75* molecules by treatment with 10 mM NaOH (see Fig. 1 *B*).

SPFS setup

The SPFS setup was constructed based on a conventional surface plasmon spectrometer, in combination with a photon counting unit (Liebermann and Knoll, 2000). The emitted fluorescence light from the sample surface was collected through a quartz flow cell. A lens ($f = 40$ mm) focused the light

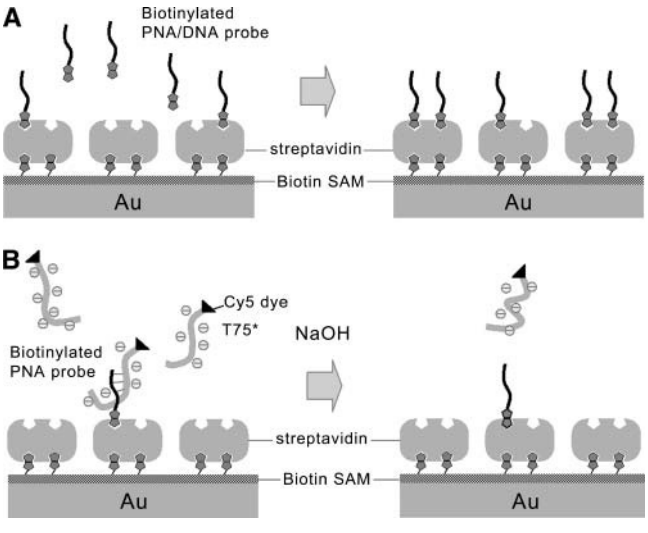

FIGURE 1 Schematic representation of the protocols used for the preparation of an undiluted PNA/DNA probe layer (*A*) and a diluted PNA probe layer (*B*), respectively.

through an interference filter ($\lambda = 670$ nm, $T = 69\%$) onto a photomultiplier tube, the signal of which was fed into a photon counter. This fluorescence detection unit was mounted on the sample stage, such that its position was fixed relative to the sample surface. Kinetic measurements were realized by recording the fluorescence intensity as a function of time.

RESULTS AND DISCUSSION

Hybridization on an undiluted PNA or DNA probe layer

Fig. 2 shows the hybridization of PCR T2 on an undiluted PNA P2 surface measured in a series of sodium concentrations ranging from 10 mM to 1 M. The relationship between ionic strength and hybridization signal was established by plotting the fluorescence signal after 1 h versus the corresponding sodium concentration (see Fig. 4). The hybridization signals were found to increase with the sodium concentration increasing from 10 mM to 100 mM, and then to decrease with sodium concentration continuously increasing.

This finding indicates that the ionic strength influenced the hybridization reaction at least in two aspects. On the one hand, in low salt concentrations, the hybridization reaction is strongly retarded by the electrostatic repulsion among the DNA molecules. As demonstrated earlier in the aqueous phase, PNA/DNA hybridization is relatively independent on the ambient ionic strength owing to the neutral backbone of PNA. However, with the PNA probes confined to the surface of a biosensor, the hybridization takes place in a constraint geometry, i.e., a two-dimensional substrate in our case, which is assumed to significantly promote cross talk between the DNA or PNA molecules. For instance, bound DNA molecules may hinder the access of free DNA molecules from solution to the surface by electrostatic repulsion, with this electrostatic cross talk being more severe for longer DNA molecules and in low salt conditions. A higher sodium concentration obviously alleviates the electrostatic cross talk by shielding the charges. On the other hand, the higher ionic strength also stabilizes the inter- and intramolecular structures of PCR amplicons. For instance, the melting temperature (T_m) of the 196-basepair PCR T2 is estimated to be ~70°C and ~97°C at 10 mM and 1 M sodium concentration, respectively. Therefore, a portion of PCR amplicons may still preserve double-stranded structure by being heated to 96°C in higher salt condition, which reduces the concentration of the effective sense strands. Consequently, as a compromise of the above two factors, the largest hybridization signal was obtained at an intermediate sodium concentration (~100 mM). These two factors were also reflected in the hybridization kinetics. By the exposure to lower salt conditions, both the resulting lower binding capacities and higher effective target concentrations led to faster association rates.

The ionic strength dependence of the PCR amplicon hybridization was also checked on a DNA probe layer by varying the sodium concentration from 10 mM to 850 mM (see Fig. 3). Compared with the PNA probe, the ionic strength effect was further enhanced. A significantly narrowed ionic strength window for maximum hybridization was found for the DNA P2 surface, as revealed in Fig. 4. Particularly, the hybridization signals within the window of 10 ~ 150 mM sodium concentration were considerably lower than those obtained on the PNA probe layer. The difference in the hybridization response to the ionic strength variation is mainly ascribed to the dissimilar electrostatic environment provided by PNA and DNA. Being initially neutral, the PNA probe surface is gradually charged by the continuous hybridization of DNA molecules. In contrast, the negatively charged DNA probe surface electrostatically repels the free DNA molecules in the bulk solution already at the early stage the hybridization. The charges carried by both DNA probe and DNA target strongly inhibit the formation of the double helix, particularly in the lower sodium concentration range. Therefore, in addition to the aforementioned electrostatic cross talk and the secondary structure of PCR amplicons, the hybridization reaction on the

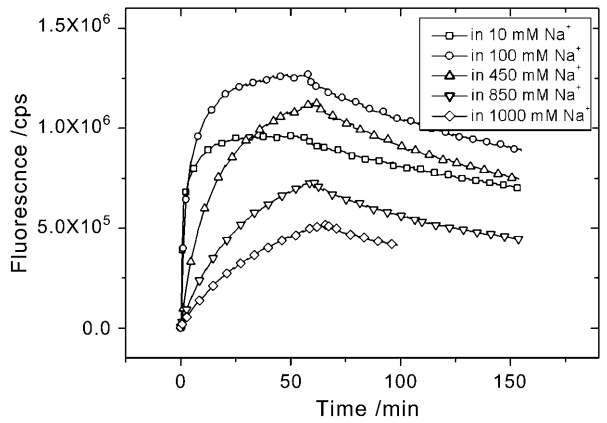

FIGURE 2 Hybridization reactions of PCR T2 (100 nM) to an undiluted PNA P2 probe surface at 10, 100, 450, 850, and 1000 mM sodium concentration, respectively. An attenuator (with the attenuation factor of 14) was applied to reduce the fluorescence intensity.

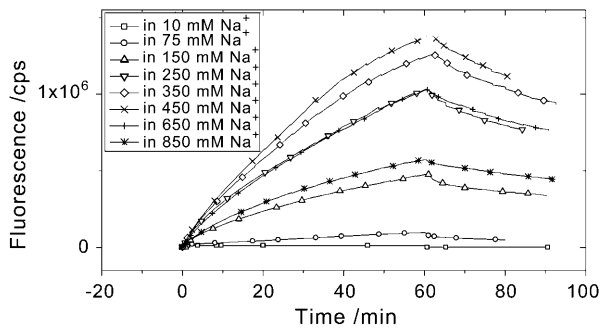

FIGURE 3 Hybridization reactions of PCR T2 (100 nM) to an undiluted DNA P2 probe surface at 10, 75, 150, 250, 350, 450, 650, and 850 mM sodium concentration, respectively. An attenuator (with the attenuation factor of 14) was applied.

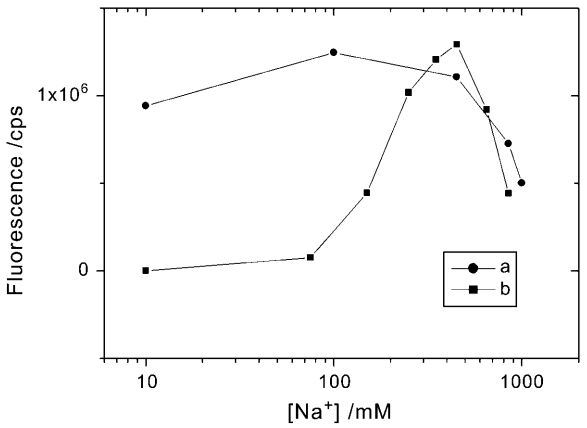

FIGURE 4 Ionic strength dependence of the hybridization response of PCR T2 after 1 h of contact with the undiluted PNA (*a*) and DNA (*b*) probe layer, extracted from the data of Figs. 2 and 3, respectively.

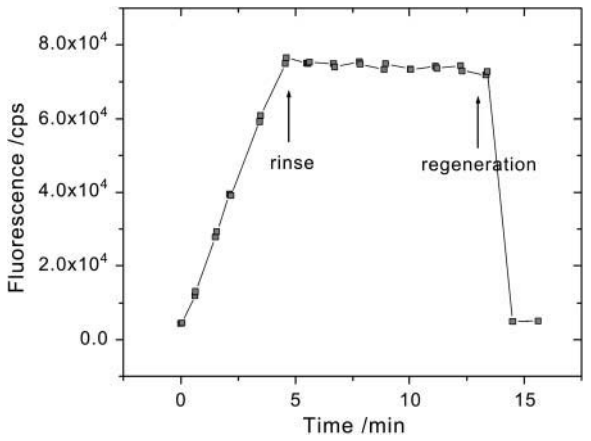

FIGURE 5 Surface assembly of the PNA P2· T75* hybrids via biotin/SA interaction at 10 mM sodium concentration, followed by treatment with NaOH solution (10 mM) for the removal of the T75* molecules.

DNA probe layer is additionally subjected to the DNA/DNA electrostatic barrier, which thus led to slower association rates and lower hybridization signals in the sodium concentration window of 10 ~ 150 mM, compared with those observed on the PNA probe layer.

Hybridization on a diluted PNA probe layer

In an effort to minimize the electrostatic cross talk and improve the hybridization efficiency, a highly diluted PNA probe layer was prepared. Strategically, several dilution methods could be applied for conventional DNA probes, such as kinetically controlling the assembly of DNA probe layer (Yu et al., 2004) or its underlying SA layer. However, unlike DNA, the neutral backbone of PNA introduces additional difficulties in achieving a homogeneously diluted layer. For instance, it is likely that in the absence of electrostatic repulsion more than two biotinylated PNA molecules bind to one tetrameric SA molecule, resulting in local crowding of PNA probes. The probability could be largely reduced by mixing a noncomplementary PNA sequence into the PNA probe solution to compete for the SA binding sites. However, the presence of the noncomplementary PNA may also cause steric hindrance in hybridization, because the overall PNA density is not reduced.

Thus, we propose a novel dilution concept in this work. Acting as a binding template, an excess of T75* was allowed to prehybridize with the PNA P2 probe in a homogeneous phase at a sodium concentration of 10 mM. Upon assembly, the PNA P2 was bound to the SA surface mostly as a hybrid with T75*, as illustrated in Fig. 1 *B*. The strong electrostatic repulsion among neighboring T75* molecules favors the even distribution of the assembled hybrids by occupying only one of the SA binding pockets. Upon removing T75* by exposing the hybrids to an alkali solution, a homogeneous PNA P2 surface was obtained. As shown in Fig. 5, the assembly of PNA P2·T75* hybrids and the removal of the T75* molecules were observed by the steady increase and the sudden vanishing of the fluorescence signal, respectively. The extremely lowered concentration of PNA P2 (300 pM) helps to establish a strictly mass-transport limited immobilization, in which the binding amount increases linearly with time. The layer density can be easily tuned by varying the concentration of the PNA P2 solution and by controlling the contact time in the assembly process.

With the diluted PNA probe layer, the ionic strength effect was again investigated. Fig. 6 *A* shows a series of hybridization kinetic runs of PCR T2 in solution with a sodium concentration varying from 10 mM to 1 M. In contrast to an undiluted probe surface, the hybridization signals exhibited a tendency of monotonic decrease with increasing ionic strength (see Fig. 6 *B*). This suggests the absence of electrostatic cross talk on the diluted surface that drives the tendency oppositely. By comparing the equilibrium fluorescence signals obtained on the undiluted and diluted surface at 10 mM sodium concentration, the PNA P2 layer was at least 40× diluted. On such a highly diluted surface, the other surface effects, such as the steric cross talk, were also assumed to be efficiently eliminated. Therefore, the monotonic decreases of the hybridization signals and of the association rates are ascribed mostly to the reduction of the effective target concentration in higher salt conditions.

SNP identification on a diluted PNA probe layer

Unlike for oligonucleotide targets, the hybridization kinetics of PCR amplicons in most cases tend to drastically deviate from the Langmuir model due to the strongly enhanced (and coverage dependent) steric/electrostatic cross talk. As a consequence, the quantitative identification of single nucleotide polymorphisms (SNPs) of PCR amplicons is mostly accomplished by evaluating the end-point response. Although the

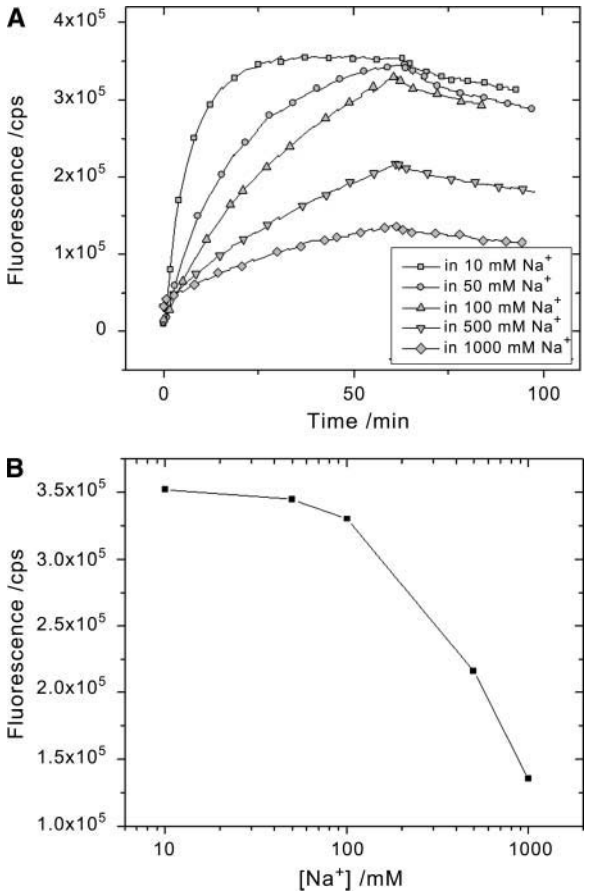

FIGURE 6 (*A*) Hybridization reactions of PCR T2 (100 nM) on the diluted PNA P2 surface at 10, 50, 100, 500, and 1000 mM sodium concentration, respectively. (*B*) Ionic strength dependence of the hybridization response of PCR T2 after 1 h of contact with the diluted PNA probe layer, as extracted from Fig. 6 *A*.

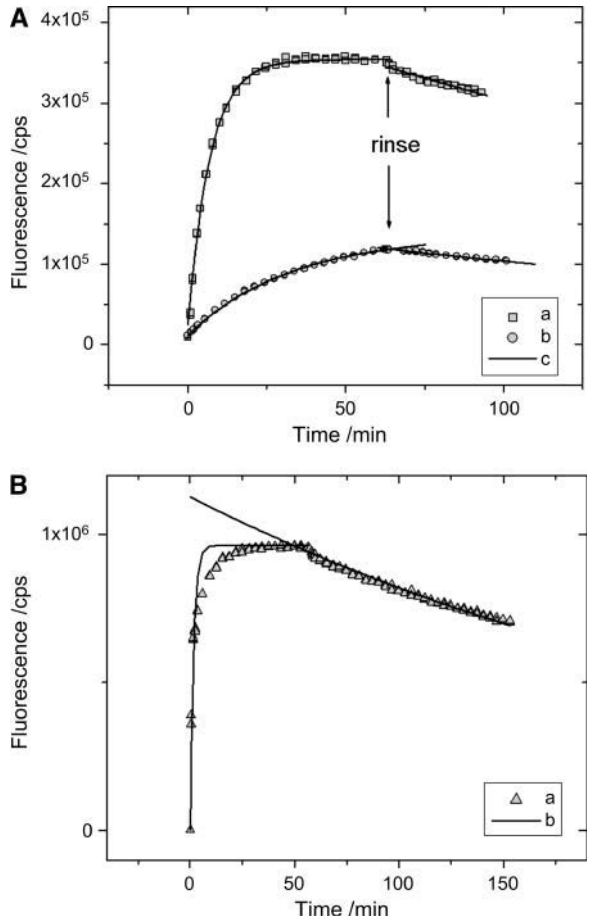

FIGURE 7 (*A*) Hybridization kinetics of PCR T2 (*a*) or PCR T1 (*b*), respectively, on the diluted PNA P2 surface at 10 mM sodium concentration. By fitting the data with a pseudo-first-order kinetic model (*c*), k_{on}, k_{off}, and K_A were accordingly derived: $2.3 \times 10^4\ M^{-1}s^{-1}$, $6.2 \times 10^{-5}\ s^{-1}$, $3.8 \times 10^8\ M^{-1}$ for PCR T2, and $4.4 \times 10^3\ M^{-1}s^{-1}$, $6.9 \times 10^{-5}\ s^{-1}$, and $6.5 \times 10^7\ M^{-1}$ for PCR T1, respectively. (*B*) Hybridization kinetics of PCR T2 (*a*) on an undiluted PNA P2 surface at 10 mM sodium concentration (extracted from Fig. 2), fitted by the kinetic model (*b*).

hybridization process can be followed by quartz crystal microbalance (QCM) (Mannelli et al., 2003), by surface plasmon resonance (SPR) (Nilsson et al., 1999; Corradini et al., 2004) or by total internal reflection fluorescence spectroscopy (TIRF) (Lehr et al., 2003), rare attempt was reported to dig out the physical meaning of the hybridization kinetics of PCR amplicons so far. In view of this, the diluted PNA probe layer was used to discriminate the SNPs in this article, on which the cross talk was largely eliminated and hence the Langmuir model might be applicable.

Fig. 7 *A* shows the results of the hybridization reactions of PCR T2 and T1, respectively, on an ~40× diluted PNA P2 surface. The hybridizations were conducted at 10 mM sodium concentration for minimizing any interference from the anti-sense strand by virtue of the enhanced DNA/DNA electrostatic repulsion (Yao et al., 2004). The significantly lowered loading capacity resulted in the one-to-one interaction between the probe and the target molecules. Moreover, kinetically, it largely eliminated any mass transport limitations. Thus, the resulting hybridization kinetics approached a common pseudo-first-order kinetic model: the association (hybridization) curves could be fitted by

$$R = R_{eq}\{1 - \exp[-(k_{on}c + k_{off})t]\}, \quad (1)$$

where R is the fluorescence response, which is proportional to the amount of hybridized PCR amplicons. R_{eq} is the equilibrium response at the target concentration c. k_{on} and k_{off} are the association and dissociation rate constant, respectively. With $c = 0$, the dissociation (rinsing) curves could be fitted by

$$R = R_{eq}\exp(-k_{off}t). \quad (2)$$

As indicated by the solid lines (see Fig. 7 *A*), the theoretical curves fit the kinetic curves quite well for both the PCR T2 and T1 hybridization. k_{on} and k_{off} can be accordingly determined, which are $2.3 \times 10^4\ M^{-1}s^{-1}$, $6.2 \times 10^{-5}\ s^{-1}$ for PCR T2, and $4.4 \times 10^3\ M^{-1}s^{-1}$, $6.9 \times 10^{-5}\ s^{-1}$ for

PCR T1, respectively. In contrast, if the kinetic curve obtained on an undiluted probe layer was fitted by the kinetic model as well, large deviations were found in the association phase (see Fig. 7 *B*), implying the presence of severe cross talk. The still acceptable fitting of the dissociation phase suggests that the dissociation process is not influenced that much by the crosstalk, but rather by the affinity of the recognition sequences (Bier and Kleinjung, 2001).

The affinity constant K_A can then be derived by

$$K_A = k_{on}/k_{off}, \quad (3)$$

which is $3.8 \times 10^8\ M^{-1}$ for PCR T2 and $6.5 \times 10^7\ M^{-1}$ for PCR T1 on the diluted probe surface, respectively. The affinity constants provide a quantitative assessment of SNPs, in addition to the simple comparison of end-point fluorescence signals. In our case, the one base mismatch (A/ C mismatch) in the recognition sequence reduces the affinity constant by a factor of ~5. Nevertheless, it is noteworthy that a small portion of the PCR amplicons may inevitably re-anneal in the quenching step, since the temperature range favorable for re-annealing (~70°C−~20°C) was passed through, even in a very short time and with the low salt condition applied. So the effective target concentration c was presumably overestimated in kinetic fitting with Eq. 1. Independent of the target concentration, the dissociation rate constant k_{off} was not influenced. If assuming the concentration c were overestimated by a factor of two, both k_{on} and K_A would be underestimated by less than a factor of two, owing to the contribution of k_{off} in the apparent association rate constant k_{ass} ($k_{ass} = k_{on} \times c + k_{off}$). But since this underestimation was equal to PCR T1 and T2, it would not have influenced the quantitative identification of SNPs. For a more precise quantification of k_{on} and K_A, the re-annealing effect can be largely eliminated by adding formamide (Sawata et al., 1999) or by removing the anti-sense strand with SA modified magnetic beads (Nilsson et al., 1997).

CONCLUSIONS

Densely packed PNA and DNA probe layers responded differently to ionic strength variations in the hybridization reactions with PCR amplicons. For the uncharged PNA probe, the ionic strength effect is mostly attributed to the stabilized secondary structure of the PCR amplicons in higher salt conditions and the electrostatic interaction occurring between the surface-hybridized DNA molecules. For the DNA probe, the ionic strength influence is more complex. Being both negatively charged, the DNA probe and the DNA target electrostatically repel each other. This strongly influences the hybridization reactions besides the two factors for PNA probes, particularly, in lower sodium concentration range (10 ~ 150 mM) and accounts for the greatly narrowed ionic strength window observed for the hybridization on the DNA probe layer. The maximum hybridization signal was achieved at ~100 mM and ~450 mM sodium concentration for the PNA and DNA probe, respectively.

Being strongly correlated with the loading capacity, the electrostatic crosstalk can be nearly completely eliminated by reducing the surface probe density. A new method was developed for achieving a homogeneous and highly diluted PNA probe surface, by virtue of the electrostatic repulsion existing among the combined DNA templates at a sodium concentration of 10 mM. The elimination of the crosstalk was indicated by a monotonic decrease of hybridization signals with the increase of the ionic strength. For this situation, the target hybridization follows the Langmuir model which allows for a quantitative interpretation of the hybridization kinetics. The affinity constants were accordingly derived and were used for a quantitative discrimination of SNPs.

This work was supported by an European Union grant (QLKI-2000-31658, ''DNA-track'').

REFERENCES

Bier, F. F., and F. Kleinjung. 2001. Feature-size limitations of microarray technology—a critical review. *Fresenius'. J. Anal. Chem.* 371:151–156.

Bier, F. F., F. Kleinjung, and F. W. Scheller. 1997. Real-time measurement of nucleic-acid hybridization using evanescent-wave sensors: steps towards the genosensor. *Sens. Actuators, B.* 38:78–82.

Corradini, R., G. Feriotto, S. Sforza, R. Marchelli, and R. Gambari. 2004. Enhanced recognition of cystic fibrosis W1282X DNA point mutation by chiral peptide nucleic acid probes by a surface plasmon resonance biosensor. *J. Mol. Recognit.* 17:76–84.

Egholm, M., O. Buchardt, L. Christensen, C. Behrens, S. M. Freier, D. A. Driver, R. H. Berg, S. K. Kim, B. Norden, and P. E. Nielsen. 1993. PNA hybridizes to complementary oligonucleotides obeying the Watson-Crick hydrogen-bonding rules. *Nature.* 365:566–568.

Epstein, J. R., I. Biran, and D. R. Walt. 2002. Fluorescence-based nucleic acid detection and microarrays. *Anal. Chim. Acta.* 469:3–36.

Herne, T. M., and M. Tarlov. 1997. Characterization of DNA probes immobilized on gold surfaces. *J. Am. Chem. Soc.* 119:8916–8920.

Lehr, H. P., M. Reimann, A. Brandenburg, G. Sulz, and H. Klapproth. 2003. Real-time detection of nucleic acid interactions by total internal reflection fluorescence. *Anal. Chem.* 75:2414–2420.

Liebermann, T., and W. Knoll. 2000. Surface-plasmon field-enhanced fluorescence spectroscopy. *Colloid. Surface. A.* 171:115–130.

Liebermann, T., W. Knoll, P. Sluka, and R. Herrmann. 2000. Complement hybridization from solution to surface-attached probe-oligonucleotides observed by surface-plasmon-field-eahanced fluorescence spectroscopy. *Colloid. Surface. A.* 169:337–350.

Mannelli, I., M. Minunni, S. Tombelli, and M. Mascini. 2003. Quartz crystal microbalance (QCM) affinity biosensor for genetically modified organisms (GMOs) detection. *Biosens. Bioelectron.* 18:129–140.

Nilsson, P., A. Larsson, J. Lundeberg, M. Uhlen, and P. A. Nygren. 1999. Mutational scanning of PCR products by subtractive oligonucleotide hybridization analysis. *Biotechniques.* 26:308–316.

Nilsson, P., B. Persson, A. Larson, M. Uhlen, and P. A. Nygren. 1997. Detection of mutations in PCR products from clinical samples by surface plasmon resonance. *J. Mol. Recognit.* 10:7–17.

Sawata, S., E. Kai, K. Ikebukuro, T. Iida, T. Honda, and I. Karube. 1999. Application of peptide nucleic acid to the direct detection of deoxyribonucleic acid amplified by polymerase chain reaction. *Biosens. Bioelectron.* 14:397–404.

Southern, E., K. Mir, and M. Shchepinov. 1999. Molecular interactions on microarrays. *Nat. Genet.* 21:5–9.

Spinke, J., M. Liley, F. J. Schmitt, H. J. Guder, L. Angermaier, and W. Knoll. 1993. Molecular recognition at self-assembled monolayers—optimization of surface functionalization. *J. Chem. Phys.* 99:7012–7019.

Yang, M. S., M. E. McGovern, and M. Thompson. 1997. Genosensor technology and the detection of interfacial nucleic acid chemistry. *Anal. Chim. Acta.* 346:259–275.

Yao, D. F., F. Yu, J. Y. Kim, J. Scholz, P. E. Nielsen, E. K. Sinner, and W. Knoll. 2004. Surface plasmon field-enhanced fluorescence spectroscopy in PCR product analysis by peptide nucleic acid probes. *Nucleic Acids Res.* 32:e177.

Yu, F., B. Persson, S. Löfas, and W. Knoll. 2004. Attomolar sensitivity in bioassays based on surface plasmon fluorescence spectroscopy. *J. Am. Chem. Soc.* 126:8902–8903.

Yu, F., D. F. Yao, and W. Knoll. 2004. Oligonucleotide hybridization studied by a surface plasmon diffraction sensor (SPDS). *Nucleic Acids Res.* 32:e75.